Response of CO2 and H2O fluxes in a mountainous tropical rainforest in equatorial Indonesia to El Niño events

Olchev, A.; Ibrom, Andreas; Panferov, O.; Gushchina, D.; Kreilein, H.; Popov, V.; Propastin, P.; June, T.; Rauf, A.; Gravenhorst, G.

Total number of authors:
11

Published in:
Biogeosciences

Link to article, DOI:
10.5194/bgd-12-4405-2015

Publication date:
2015

Document Version
Publisher's PDF, also known as Version of record

Biogeosciences, 12, 6655–6667, 2015
www.biogeosciences.net/12/6655/2015/
doi:10.5194/bg-12-6655-2015

Biogeosciences Open Access EGU

Response of CO_2 and H_2O fluxes in a mountainous tropical rainforest in equatorial Indonesia to El Niño events

A. Olchev[1,2], A. Ibrom[3], O. Panferov[4], D. Gushchina[5], H. Kreilein[2], V. Popov[6,7], P. Propastin[2], T. June[8], A. Rauf[9], G. Gravenhorst[*], and A. Knohl[2]

[1]A.N. Severtsov Institute of Ecology and Evolution of RAS, Moscow, Russia
[2]Department of Bioclimatology, Faculty of Forest Sciences and Forest Ecology, Georg August University of Goettingen, Goettingen, Germany
[3]Department for Environmental Engineering, Technical University of Denmark, Kgs. Lyngby, Denmark
[4]Climatology and Climate Protection, Faculty of Life Sciences and Engineering, University of Applied Sciences, Bingen am Rhein, Germany
[5]Department of Meteorology and Climatology, Faculty of Geography, Moscow State University, Moscow, Russia
[6]Faculty of Physics, Lomonosov Moscow State University, Moscow, Russia
[7]Financial University under the Government of the Russian Federation, Moscow, Russia
[8]Bogor Agricultural University, Department of Geophysics and Meteorology, Bogor, Indonesia
[9]Universitas Tadulako, Palu, Indonesia
[*]retired

Correspondence to: A. Olchev (aoltche@gmail.com)

Received: 8 February 2015 – Published in Biogeosciences Discuss.: 16 March 2015
Revised: 30 September 2015 – Accepted: 6 November 2015 – Published: 24 November 2015

Abstract. The possible impact of El Niño–Southern Oscillation (ENSO) events on the main components of CO_2 and H_2O fluxes between the tropical rainforest and the atmosphere is investigated. The fluxes were continuously measured in an old-growth mountainous tropical rainforest in Central Sulawesi in Indonesia using the eddy covariance method for the period from January 2004 to June 2008. During this period, two episodes of El Niño and one episode of La Niña were observed. All these ENSO episodes had moderate intensity and were of the central Pacific type. The temporal variability analysis of the main meteorological parameters and components of CO_2 and H_2O exchange showed a high sensitivity of evapotranspiration (ET) and gross primary production (GPP) of the tropical rainforest to meteorological variations caused by both El Niño and La Niña episodes. Incoming solar radiation is the main governing factor that is responsible for ET and GPP variability. Ecosystem respiration (RE) dynamics depend mainly on the air temperature changes and are almost insensitive to ENSO. Changes in precipitation due to moderate ENSO events did not have any notable effect on ET and GPP, mainly because of sufficient soil moisture conditions even in periods of an anomalous reduction in precipitation in the region.

1 Introduction

The contribution of tropical rainforests to the global budget of greenhouse gases, their possible impact on the climatic system, and their sensitivity to climatic changes are key topics of numerous theoretical and experimental studies (Clark and Clark, 1994; Grace et al., 1995, 1996; Malhi et al., 1999; Ciais et al., 2009; Lewis et al., 2009; Phillips et al., 2009; Malhi, 2010; Fisher et al., 2013; Moser et al., 2014). The area covered by tropical rainforests was drastically reduced during the last century, mainly due to human activity, and presently there are less than 11.0 million km^2 remaining (Malhi, 2010). While deforestation rates in the tropical forests of Brazil are now declining, countries in southeast Asia, particularly Indonesia, show the largest increase in forest loss globally (FAO, 2010; Hansen et al., 2013), resulting in major changes in carbon and water fluxes between the

land surface and the atmosphere. Therefore, during the last decade the tropical forest ecosystems of southeast Asia and especially Indonesia are the focus area of intensive studies of biogeochemical cycle and land-surface–atmosphere interactions. It is necessary to know, on the one hand, how these tropical forests influence the global and regional climate, and on the other hand, how they respond to changes in regional climatic conditions.

Climate and weather conditions in the equatorial Pacific and southeastern part of Asia are mainly influenced by the Intertropical Convergence Zone (ITCZ) which is seasonally positioned north and south of the Equator. Another very important factor affecting the climate of southeast Asia is the well-known coupled oceanic and atmospheric phenomenon, El Niño–Southern Oscillation (ENSO). During the warm phase of ENSO, termed "El Niño", sea surface temperature (SST) in the central and eastern parts of the equatorial Pacific sharply increases, and during a cold phase of the phenomenon, termed "La Niña", the SST in these areas is lower than usual. Both phenomena, El Niño and La Niña, lead to essential changes in pressure distribution and atmospheric circulation and, as a result, to anomalous changes in precipitation amount, solar radiation, and temperature fields, both in the regions of sea surface temperature anomalies and in a wide range of remote areas through the mechanism of atmospheric bridges (Wang, 2002; Graf and Zanchettin, 2012; Yuan and Yan, 2013). Typically, in Indonesia El Niño results in dryer conditions and La Niña results in wetter conditions, potentially impacting the land vegetation (Erasmi et al., 2009). ENSO events are irregular, characterized by different intensities and, are usually observed at intervals of 2–7 years.

To describe the possible effects of ENSO events on the CO_2 and H_2O exchange between the land surface and the atmosphere, many studies for different western Pacific regions were carried out during recent decades (Feely et al., 1999; Malhi et al., 1999; Rayner and Law, 1999; Aiba and Kitayama, 2002; Hirano et al., 2007; Erasmi et al., 2009; Gerold and Leemhuis, 2010). They are mainly based on the results of modeling experiments and remote-sensing data (Rayner and Law, 1999). Experimental results based on the direct measurements of CO_2 and H_2O fluxes, which allow studying the response of individual terrestrial ecosystems to anomalous weather conditions, are still very limited (e.g., Hirano et al., 2007; Moser et al., 2014). Existing monitoring networks in equatorial regions of the western Pacific are associated mainly with lowland areas and do not cover mountainous rainforest regions, even though mountainous regions cover some of the last remaining undisturbed rainforest in southeast Asia. Most attention in previous studies was paid to the description of plant response to anomalously dry and warm weather during El Niño events (Aiba and Kitayama, 2002; Hirano et al., 2007; Moser et al., 2014). The possible changes in plant functioning during La Niña events have not yet been clarified. In particular, Malhi et al. (1999) reported that for the Amazon region in South America, El Niño periods are strongly associated with enhanced dry seasons that probably result in increased carbon loss, either through water stress causing reduced photosynthesis or increased tree mortality. Aiba and Kitayama (2002) examined the effects of the 1997–1998 El Niño drought on nine rainforests of Mount Kinabalu in Borneo using forest inventory and showed that El Niño increased the tree mortality for lowland forests. However, it did not affect the growth rate of the trees in upland forests (higher than 1700 m) where mortality was restricted by some understorey species only. Eddy covariance measurements of the CO_2 fluxes in a tropical peat swamp forest in Central Kalimantan, Indonesia, for the period from 2002 to 2004, provided by Hirano et al. (2007), showed that during the El Niño event in the period November–December 2002, the annual net CO_2 release reached maximal values, mainly due to a strong decrease of GPP in the late dry season because of dense smoke emitted from large-scale fires. The effects of El Niño on annual ecosystem respiration (RE) in 2002 were insignificant.

There is a lack of experimental data on CO_2 and H_2O fluxes in mountainous rainforests in equatorial regions of the western Pacific and on their response to ENSO. Hence, the main objective of this study was to evaluate and quantify the impact of ENSO events on the main components of CO_2 and H_2O fluxes in an old-growth mountainous tropical rainforest in Central Sulawesi, Indonesia. The methodology used was the analysis of long-term eddy covariance flux measurement data.

2 Materials and Methods

2.1 El Niño's types and intensity

Today, two types of ENSO can be distinguished: (1) the canonical or conventional El Niño, which is characterized by SST anomalies located in the eastern Pacific near the South American coast (Rasmusson and Carpenter, 1982), and (2) the central Pacific El Niño or El Niño Modoki (Larkin and Harrison, 2005; Ashok et al., 2007; Kug et al., 2009; Ashok and Yamagata, 2009; Gushchina and Dewitte, 2012). In 2003, a new definition of the conventional El Niño was accepted by the National Oceanic and Atmospheric Administration (NOAA) of the USA, in referring to the warming of the Pacific region between 5° N–5° S and 170–120° W. According to Ashok et al. (2007) the central Pacific El Niño, or El Niño Modoki, – i.e., unusually high SST – occurs roughly in the region between 160° E–140° W and 10° N–10° S.

As criteria to assess the intensity of ENSO events, a wide range of indexes based on different combinations of sea level pressure and SST data in various areas of the Pacific is used. For diagnostics of the central Pacific El Niño, the SST anomalies (in °C) in the Nino4 region (5° N–5° S and 160° E–150° W) are commonly used (Fig. 1). The monthly SST anomalies (in °C) in the Nino3.4 region (5° N–5° S and

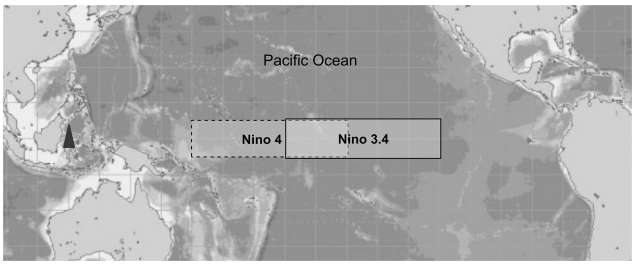

Figure 1. Geographical location of the study area (marked by black triangle) in tropical rain forest in Central Sulawesi (Indonesia) and Nino4 and Nino3.4 regions.

170–120° W) are used to diagnose both types of El Niño phenomenon: canonical and central Pacific (Download Climate Timeseries, 2013).

2.2 Experimental site

The tropical rainforest selected for the study is situated near the village of Bariri in the southern part of the Lore Lindu National Park of Central Sulawesi in Indonesia (1°39.47′ S and 120°10.409′ E or UTM 51S 185482 M east and 9816523 M north) (Fig. 1). The site is located on a large plateau of several kilometers in size at about 1430 m above sea level surrounded by mountain chains rising above the plane by another 300 to 400 m. Within 500 m around the tower the elevation varies between 1390 and 1430 m. Wind field measurement with a sonic anemometer indicate a slope of around 2–3°, which is similar to many FLUXNET sites. About 1000 m to the east of the experimental site, the forest is replaced by a meadow; in all other directions it extends for several kilometers (Ibrom et al., 2007).

According to the Köppen climate classification the study area relates to tropical rainforest climate (*Af*) (Chen and Chen, 2013). Weather conditions in the region are mainly influenced by the ITCZ. During the wet season (typically, from November to April), the area is influenced by very moist northeast monsoons coming from the Pacific. Maximum precipitation during the observation period from January 2004 to July 2008 was observed in April – with 258.0 ± 148.0 mm month^{-1}. The drier season usually lasts from May to October. The precipitation minimum was observed in September with 195.0 ± 48.0 mm month^{-1}. The September–October period was also characterized by maximal incoming solar radiation, up to 650 ± 47.0 MJ m^{-2} month^{-1}, mainly because of a significant decrease in convective clouds, due to the reversing of an oceanic northeast monsoon to a southeast monsoon blowing from the Australian continent. The mean annual precipitation amount exceeded 2000 mm. The mean monthly air temperature varies between 19.4 and 19.7 °C. The mean annual air temperature was 19.5 °C (Falk et al., 2005; Ibrom et al., 2007).

The vegetation at the experimental site is very diverse and representative of the mountainous rainforest communities of Central Sulawesi. There are about 88 different tree species per hectare. Among the dominant species are *Castanopsis accuminatissima* BL. (29 %), *Canarium vulgare* Leenh. (18 %) and *Ficus spec.* (9.5 %). The density of trees, with diameter at breast height larger than 0.1 m, is 550 trees per ha. In addition, there is more than times that number of smaller trees per hectare with a stem diameter smaller than 0.1 m. The total basal area of trees reached 53 m^2 per ha. Leaf area index (LAI) is about 7.2 m^2 m^{-2}. LAI was estimated using an indirect hemispherical photography approach with a correction for leaf clumping effects. The height of the trees, with diameters at breast height larger than 0.1 m, varies between the lowest at 12 m and the highest at 36 m. The mean tree height is 21 m (Ibrom et al., 2007).

2.3 Flux measurements and gap filling

CO_2 and H_2O fluxes were measured from 2004 to 2008 within the framework of the STORMA project (Stability of Rainforest Margins in Indonesia, SFB 552), supported by the German Research Foundation (DFG). Eddy covariance equipment for flux measurements was installed on a meteorological tower of 70 m height at 48 m, i.e., ca. 12 m higher than the maximal tree height. The measuring system consists of a three-dimensional sonic anemometer (USA-1, Metek, Germany) and an open-path CO_2 and H_2O infrared gas analyzer (IRGA, LI-7500, LI-COR, USA) (Falk et al., 2005; Ibrom et al., 2007; Panferov et al., 2009). The open-path IRGA was chosen due to its smaller power requirements compared to closed-path sensors. The sensor was calibrated with calibration gases two times per year and showed no considerable sensitivity drift within 1 year of operation. Turbulence data were sampled at 10 Hz and stored as raw data on an industrial mini PC (Kontron, Germany). All instruments were powered by batteries, which were charged by solar panels, mounted on the tower. The system is entirely self-sustaining and has been proven to run unattended over a period of several months. Post-field data processing on eddy covariance flux estimates was carried out strictly according to the established recommendations for data analysis (Aubinet et al., 2012). In addition to the procedures described in Falk et al. (2005) and Ibrom et al. (2007), we corrected the flux data for CO_2 or H_2O density fluctuations due to heat conduction from the open-path sensor (Burba et al., 2008; Järvi et al., 2009) using the suggested method as described in Reverter et al. (2011).

The system operated ca. 70 % of the time. About 30 % of the measured flux data were negatively affected by rain and other unfavorable conditions and removed. From nighttime ecosystem respiration data, a friction velocity (u_*) threshold value of 0.25 m s^{-1} was estimated (Aubinet et al., 2000), i.e., at u_* values above this threshold the measured nighttime flux became independent of u_*. Nighttime flux values that were measured at $u_* < 0.25$ m s^{-1} were removed, which left 15 %

of the measured nighttime flux data in the data set. In order to fill the gaps in the measured net ecosystem exchange (NEE) and evapotranspiration, net radiation and sensible and latent heat flux records as well as to quantify GPP, RE and forest canopy transpiration, the process-based Mixfor-SVAT model (Olchev et al., 2002, 2008) was used.

Mixfor-SVAT is a one-dimensional model of the energy, H_2O and CO_2 exchange between vertically structured mono- or multi-specific forest stands and the atmosphere. The main model advantage is its ability both to describe seasonal and daily patterns of CO_2 and H_2O fluxes at individual tree and entire ecosystem levels and to estimate the contributions of soil, different forest layers, and various tree species to the total ecosystem fluxes taking into account individual structure, biophysical properties and responses of plant species to changes in environmental conditions. The model also allows us to take into account the non-steady-state water transport in the trees, rainfall interception, dew generation, turbulence and convection flows within the canopy and plant canopy energy storage. As model input the measured meteorological variables (air temperature, water vapor pressure, wind speed, precipitation, CO_2 concentration, global solar radiation) are used. The model was tested with long-term meteorological and flux data from different experimental sites including the investigated forest under well-developed turbulent conditions and showed a good agreement over a broad spectrum of weather and soil moisture conditions (Olchev et al., 2002, 2008; Falk et al., 2005; Falge et al., 2005). Using the model is superior to common statistical gap-filling approaches because these depend on calibration under all relevant weather conditions, including those that were systematically excluded when the open-path sensor did not work, e.g., under rain. For this reason one might argue that statistical gap filling is biased by calibration during dry weather conditions. The process-based model is, however, able to take these weather situations into account because it is based on general physical principles. As was shown in previous studies, the model is able to predict both CO_2 and water fluxes under various weather and soil moisture conditions at sites where closed-path sensors were used (Oltchev et al., 1996; Falge et al., 2005).

2.4 Micrometeorological measurements

Air temperature, relative humidity and horizontal wind speed were measured at four levels above and at two levels inside the forest canopy using ventilated and sheltered thermo-hygrometers and cup anemometers (Friedrichs Co., Germany) installed on the tower. Short- and long-wave radiation components were measured below and above the canopy with CM6B and CG1 sensors (Kipp & Zonen, The Netherlands). Rainfall intensity was measured on top of the tower with a tipping bucket in a Hellman-type rain gauge. To fill the gaps in measuring records the meteorological data from an automatic meteorological station, situated about 900 m away from the tower outside the forest on a nearby meadow, were used. For the analysis, the monthly mean air temperature values and monthly sums of precipitation and solar energy were calculated.

2.5 Data analysis

To estimate the possible impact of ENSO events on CO_2 and H_2O fluxes in the tropical rainforest at Bariri the temporal variability in monthly NEE, GPP, RE and ET in periods with different ENSO intensity was analyzed. To quantify the ENSO impacts on meteorological parameters and fluxes and to distinguish them from effects caused by the seasonal migration of the ITCZ, the intra-annual patterns of CO_2 and H_2O fluxes as well as meteorological conditions during the measuring period were also evaluated.

In the first step, to assess the possible impact of ENSO events on meteorological parameters (global solar radiation (G), precipitation amount (P), air temperature (T) and CO_2 and H_2O fluxes), the correlation between the absolute values of monthly G, P, T, NEE, GPP, RE, ET and monthly SST anomalies in the Nino4 and Nino3.4 regions (Nino4 and Nino3.4 indexes) were analyzed.

In the second step, we analyzed the correlation between the deviations of monthly meteorological parameter and flux values from their monthly averages over the entire measuring period and the Nino4 and Nino3.4 indexes. The deviation in the case of GPP (ΔGPP) was estimated as

$$\Delta \mathrm{GPP}_{\mathrm{Month,\ Year}} = \mathrm{GPP}_{\mathrm{Month,\ Year}} - \frac{1}{N}\sum_{\mathrm{Year}=2004}^{2008} \mathrm{GPP}_{\mathrm{Month,\ Year}}, \quad (1)$$

where $\mathrm{GPP}_{\mathrm{Month,Year}}$ is total monthly GPP for a particular month (January to December) and corresponding year (2004 to 2008); $\frac{1}{N}\sum_{\mathrm{Year}=2004}^{2008}\mathrm{GPP}_{\mathrm{Month,\ Year}}$ is monthly GPP for this particular month averaged for the entire measuring period (2004 to 2008); N is number of years. Positive values in ΔGPP, ΔRE, and ΔNEE indicate GPP, RE higher and NEE (carbon uptake) lower than average.

The typical timescale of the full ENSO cycle is estimated to be about 48–52 months (Setoh et al., 1999), whereas the timescale of the main meteorological parameters (global solar radiation (G), precipitation amount (P), air temperature (T)) is characterized by much higher month-to-month variability even after annual trend filtering. In order to filter the high-frequency oscillation in the time series of atmospheric characteristics and monthly NEE, GPP, RE, and ET anomalies, the simple centered moving average smoothing procedure was applied. The moving averages (MAs) of variables were calculated over 7 months (centered value $\pm$3 months).

Statistical analysis included both simple correlation and cross-correlation analysis (Chatfield, 2004). Cross-correlation analysis was used to take into account the possible forward and backward time shifts in maximal anomalies of meteorological parameters and CO_2 and H_2O fluxes

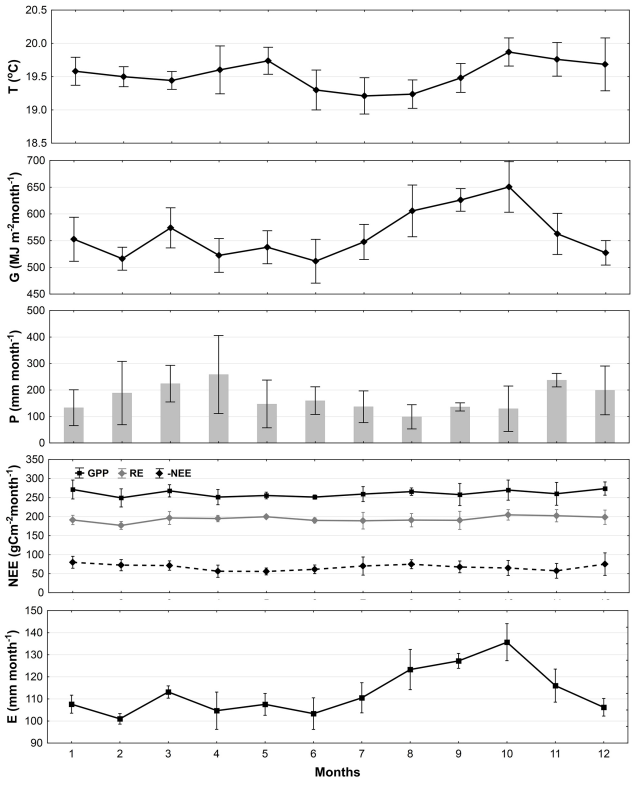

Figure 2. Mean intra-annual values of air temperature (T), global solar radiation (G), precipitation (P), NEE, GPP, RE and ET for the tropical rain forest in Bariri. Vertical whiskers indicate standard deviations (SD).

in respect to time of the ENSO culmination. To describe the relationships between atmospheric fluxes and meteorological parameters, the monthly non-smoothed values were used.

3 Results

During the measuring period, two El Niño (August 2004–March 2005 and October 2006–January 2007) and one La Niña (November 2007–April 2008) phenomena were observed. All events had moderate intensity. Both warm events could be classified as the central Pacific or Modoki type, according to Ashok et al. (2007), since the SST anomalies were centered in Nino3.4 and Nino4 regions (Fig. 1).

Analysis of the intra-annual pattern of CO_2 and H_2O fluxes shows a relatively weak seasonal variability (Fig. 2). The maximal values of GPP were obtained during the second part of the drier season – from August to October ($278 \pm 13\,g\,C\,m^{-2}\,month^{-1}$) – which is also characterized by maximal values of incoming solar radiation. The mean monthly air temperature in the period varied from minimal values in August ($19.2 \pm 0.2\,°C$) to maximal values in October ($19.8 \pm 0.2\,°C$). The minimal GPP values were obtained in transition periods between wetter and drier seasons – in May–June and November–December (240 ± 15 and $249 \pm 21\,g\,C\,m^{-2}\,month^{-1}$, respectively). These periods are also characterized by minimal amounts of incoming solar radiation ($512 \pm 40\,MJ\,m^{-2}\,month^{-1}$). Maximal RE ($206 \pm 10\,g\,C\,m^{-2}\,month^{-1}$) values were obtained in October, which corresponds to the period of maximal air temperature and insolation. The local maximum of RE in April–May ($199 \pm 4\,g\,C\,m^{-2}\,month^{-1}$) is also well correlated with a small increase in the air temperature in these months. The minimal RE was observed in February and June–August (174 ± 10 and $187 \pm 15\,g\,C\,m^{-2}\,month^{-1}$, respectively). The intra-annual pattern of ET was closely related to the seasonal variability in GPP. The maximum values of ET were also observed in October (136 ± 4 mm), in the month of maximal incoming solar radiation and highest air temperature values. In spite of a large amount of precipitation and a high air temperature during the period from March to June, ET in this period was much lower than in September and October (e.g., 105 ± 8 mm in April).

Comparisons of monthly NEE, GPP, RE, ET and absolute values of SST anomalies in the Nino4 and Nino3.4 regions (henceforth Nino4 and Nino3.4 indexes) indicate relatively low correlations. Changes in the Nino4 index can explain about 12 % of the observed variability in GPP (coefficient of determination, $r^2 = 0.12$ at significance level $p<0.05$), 9 % of RE ($r^2 = 0.09$, $p<0.05$), 9 % of NEE ($r^2 = 0.09$, $p>0.05$), 6 % of ET ($r^2 = 0.06$, $p<0.05$) and only about 1 % of transpiration (TR) ($r^2 = 0.01$, $p>0.05$). Similar values were obtained for the Nino3.4 index. In the periods of El Niño peak phases (September 2004–January 2005 and October 2006–January 2007) the values for ET and GPP tend to increase in the study area. An increase in RE was indicated only during the second El Niño event from October 2006 to January 2007. The effect of El Niño on NEE was insignificant. The effect of La Niña on CO_2 and H_2O flux components was very small and manifested itself only in a slight increase in NEE.

Analysis of the temporal variability in the centered moving average values of ΔGPP (ΔGPP_{MA}) (Fig. 3) in contrast to comparisons of absolute monthly GPP indicates a relatively high correlation between ΔGPP_{MA} and both Nino4 ($r^2 = 0.52$, $p<0.05$) and Nino3.4 ($r^2 = 0.60$, $p<0.05$) indexes. Close correlation between the intensity of ENSO events and ΔGPP_{MA} can be explained by the influence of ENSO-initiating processes and ENSO itself on total cloud amount in the region and, as a result, on monthly sums of incoming G (Fig. 4). Variability in G (ΔG_{MA}) is very closely correlated with Nino4 and Nino3.4 indexes ($r^2 = 0.48$, $p<0.05$ for both indexes) (Fig. 4) and it can explain 69 % of variability in GPP ($r^2 = 0.69$, $p<0.05$). The maximal deviations of ΔGPP_{MA} and ΔG_{MA} from mean values (averaged for the entire measuring period) occur 2–3 months before the peak phase of the ENSO events (Fig. 5). The maximal cross-correlation coefficients in this period reached 0.76 for ΔG_{MA} and 0.86 – for

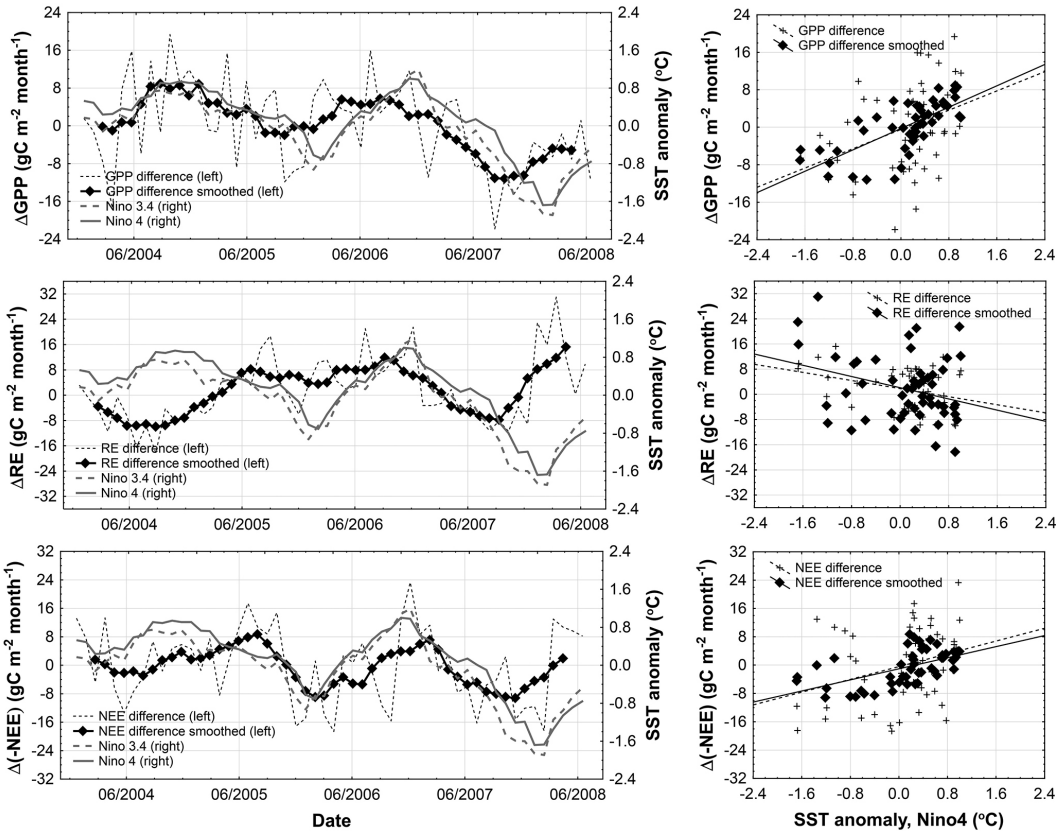

Figure 3. Comparisons of interannual patterns of SST anomalies in Nino4 and Nino3.4 zones of the equatorial Pacific with variability in both deviations and 7-month (±3 months) moving average deviations of monthly GPP, RE and NEE values from mean monthly values of GPP, RE and NEE averaged over the entire measuring period from 2004 to 2008.

ΔGPP_{MA}. The effect of T changes (ΔT) on ΔGPP is very low ($r^2 = 0.01$, $p > 0.05$).

The correlation between ΔT_{MA} and Nino4 and Nino3.4 indexes is relatively low ($r^2 = 0.15$, $p > 0.05$ for Nino4 and $r^2 = 0.05$, $p > 0.05$ for Nino3.4), and it can explain the very weak correlations between ΔRE_{MA} and ENSO indexes ($r^2 = 0.10$, $p < 0.05$ for Nino4 and $r^2 = 0.04$, $p > 0.05$ for Nino3.4) (Figs. 3–4). The maximal deviations of T_{MA} and RE_{MA} from mean values (averaged for the entire measuring period) occur 2 months after the peak phase of the ENSO events and have a negative sign (Fig. 5). The cross-correlation coefficient in this period is -0.53 ($p < 0.05$).

Despite the relatively close dependence of ΔGPP_{MA} on ENSO intensity, the correlations between ΔNEE_{MA} and Nino4 and Nino3.4 indexes are lower ($r^2 = 0.31$, $p < 0.05$ for Nino4 and $r^2 = 0.37$, $p < 0.05$ for Nino3.4), mainly because of their very low correlation during the first part of the measuring period (before December 2005). During the second part of the considered period (from June 2006 to June 2008), with one strong El Niño (October 2006–January 2007) and one La Niña (November 2004–April 2008) event, ΔNEE_{MA} and Nino4 and Nino3.4 indexes are correlated much better. This can be explained by the influence of ΔRE_{MA} on ΔNEE_{MA} dynamics, which are mainly governed by temperature variability and which is, as already mentioned, very poorly correlated with Nino4 and Nino3.4 indexes (Figs. 3–4).

Taking into account that the monthly anomalies of NEE might be biased by nighttime advection effects still unaccounted for, despite u_* filtering, we additionally examined NEE at midday (10:00–14:00 WITA), when turbulent mixing is typically well developed. Data analysis based on midday NEE shows a similarly clear relationship with the ENSO index (Fig. 6) with $r^2 = 0.59$ under $p < 0.05$. The maximal deviations of both NEE_{MA} and midday NEE_{MA} from the their mean values occurred simultaneously within the peak phase of the ENSO events (Fig. 5).

Analysis of the temporal variability in the moving average values of monthly ET (ΔET_{MA}) showed a high correlation with ENSO activity as well: $r^2 = 0.72$, $p < 0.05$ for Nino4 and $r^2 = 0.70$, $p < 0.05$ for Nino3.4 (Fig. 7), probably also triggered by G_{MA}, which in turn correlated strongly with both the Nino4 and the Nino3.4 index. Periods of extreme ΔET_{MA} values and maximal ENSO intensity occurred simultaneously (Fig. 5). Correlations between ΔET and ΔT, as well as between ΔET and ΔP, are insignificant

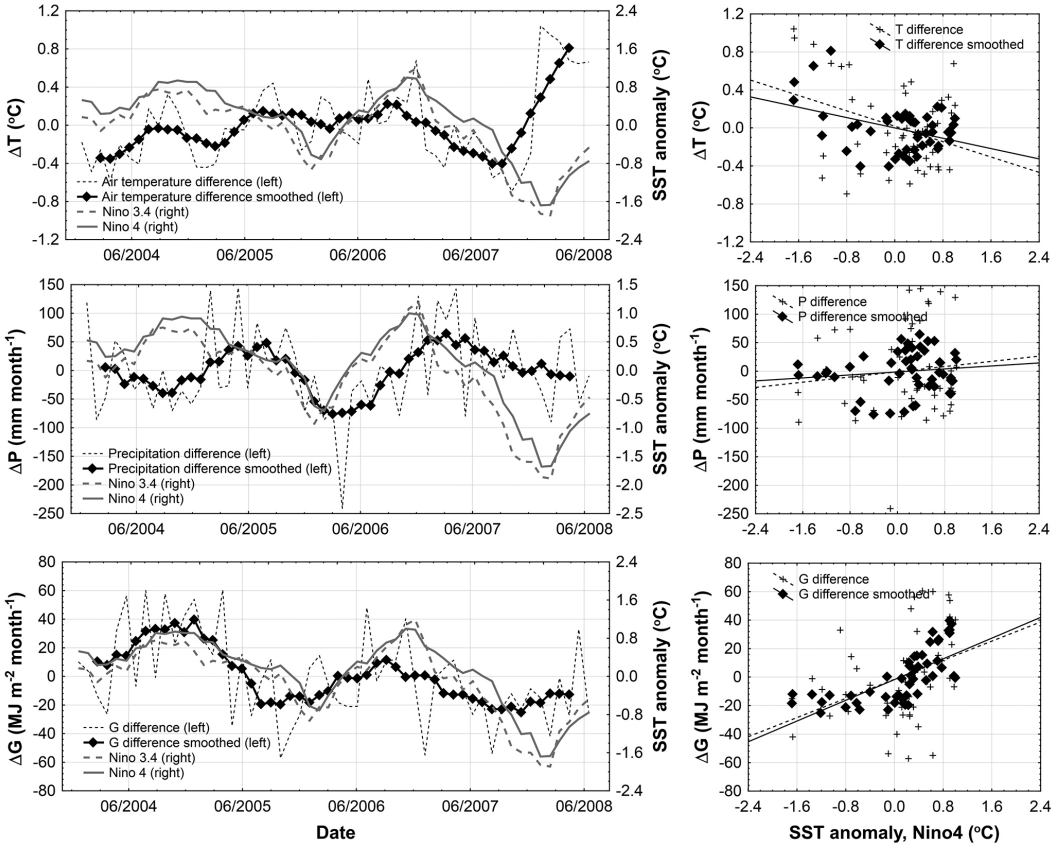

Figure 4. Comparisons of interannual patterns of SST anomalies in Nino4 and Nino3.4 zones of the equatorial Pacific with variability in both deviations and 7-month (±3 months) moving average deviations of monthly air temperature (T), precipitation (P) and global radiation (G) values from mean monthly values of T, P and G averaged over the entire measuring period from 2004 to 2008.

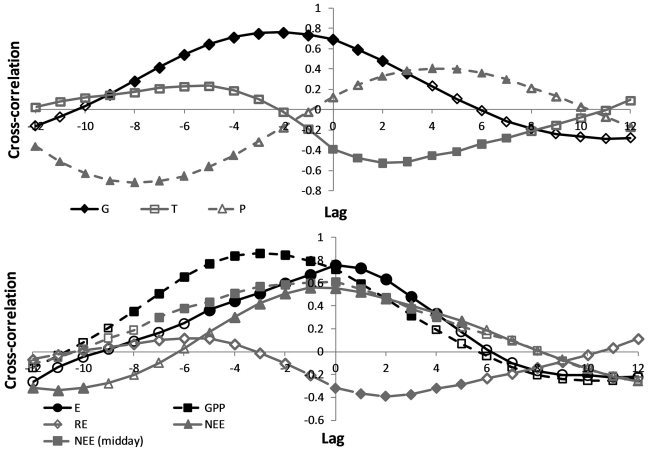

Figure 5. Cross-correlation functions between ΔG_{MA}, ΔT_{MA}, ΔP_{MA}, ΔE_{MA}, ΔGPP_{MA}, ΔRE_{MA}, ΔNEE_{MA} and midday ΔNEE_{MA} values and SST anomalies in the Nino4 zone of the equatorial Pacific. Filled symbols correspond to p value < 0.05 and non-filled symbols – to $p > 0.05$. The time lag is expressed in months.

– $r^2 = 0.09$ ($p > 0.05$) and $r^2 = 0.01$ ($p > 0.05$), respectively. However, Figs. 4 and 5 clearly show a time delay in ΔP_{MA} oscillation relative to Nino4 and Nino3.4 patterns. The maximal negative deviations of ΔP_{MA} are observed about 8 months before (cross correlation between ΔP_{MA} and Nino 4 index 0.72, $p < 0.05$) and the maximal positive deviation of ΔP_{MA} – about 4–5 months after the peak phases of ENSO (cross correlation between ΔP_{MA} and Nino 4 index – 0.40, $p < 0.05$).

To explain a very low sensitivity of ET to P changes, we analyzed the intra-annual variability in the ratio between ET and potential evaporation (PET), as well as between ET and P. PET was derived using the well-known Priestley and Taylor (1972) approach, and it is equal to evaporation from wet ground or open-water surface.

The mean annual ET during the measuring period is considerably lower than P ($ET / P = 0.742$). Annually, the ratio varied between 0.58 (in March and November) to 1.85 (in August and October). During dry periods before the positive phase of ENSO, the mean values of the ET / P ratio grew up to 1.9–2.1. During the periods of negative Nino4 and Nino3.4 anomalies, the mean monthly ET / P ratio fell, in some

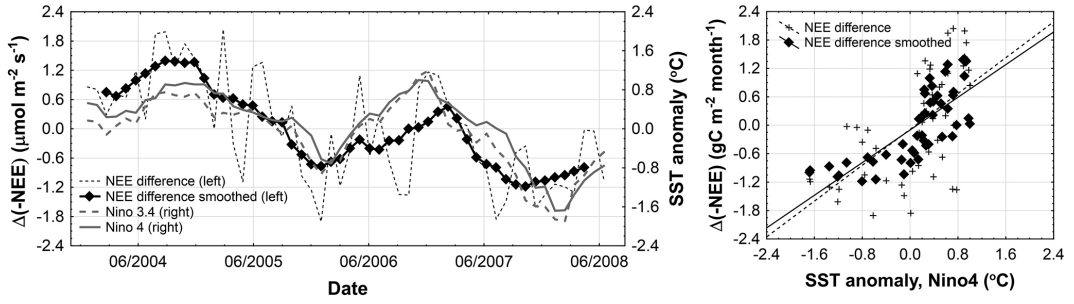

Figure 6. Comparisons of interannual patterns of SST anomalies in Nino4 and Nino3.4 zones of the equatorial Pacific with variability in both deviations and 7-month (±3 months) moving average deviations of midday NEE (10:00–14:00 WITA) values from mean monthly midday values of NEE averaged over the entire measuring period from 2004 to 2008.

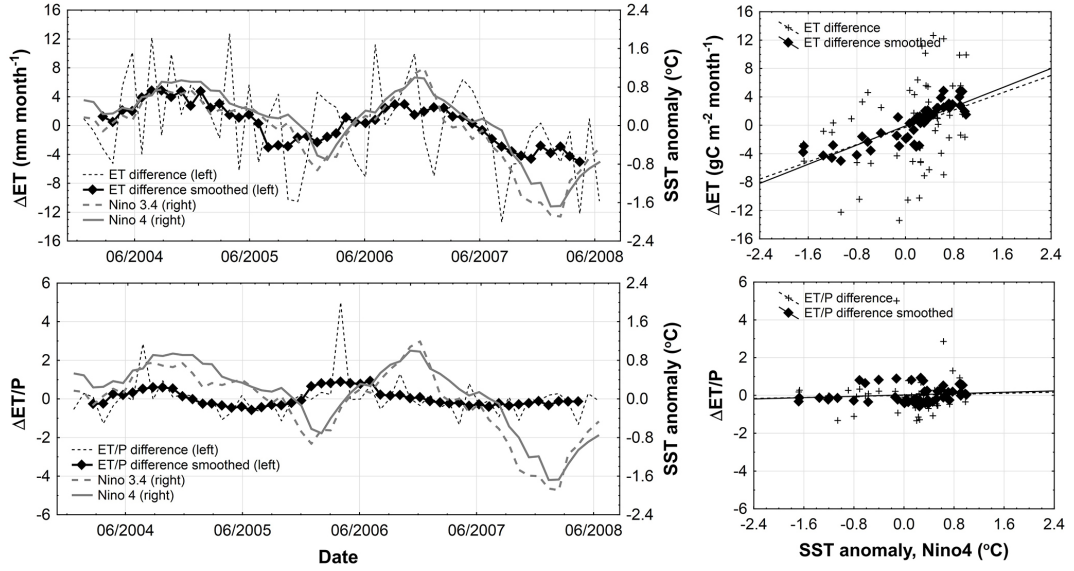

Figure 7. Comparisons of interannual patterns of SST anomalies in Nino4 and Nino3.4 zones of the equatorial Pacific with variability in both deviations and 7-month (±3 months) moving average deviations of monthly ET rate and ratio ET / P from mean monthly ET rate and ET / P averaged over the entire measuring period from 2004 to 2008.

months, down to 0.3. Correlation analysis of the temporal variability in $\Delta(\mathrm{ET}/P)$ and $\Delta(\mathrm{ET}/P)_{\mathrm{MA}}$ ratios and Nino4 and Nino3.4 indexes (Fig. 7) did not show any statistically significant relationships. However, it should be mentioned that the temporal pattern of $\Delta(\mathrm{ET}/P)$ and $\Delta(\mathrm{ET}/P)_{\mathrm{MA}}$ is characterized by two peaks that were observed in July 2005 and April 2007, about 6–8 months prior to the El Niño culmination (Fig. 7).

The monthly mean ET / PET ratio has a weak intra-annual development with a maximum in June (0.93 ± 0.03) and with minima in February and October (0.84 ± 0.06). The averaged annual ET / PET ratio for the entire measuring period was 0.880 ± 0.055. The minimal values of $(\mathrm{ET}/\mathrm{PET})_{\mathrm{MA}}$ ($(\mathrm{ET}/\mathrm{PET})_{\mathrm{MA}} = 0.81$) were observed during the El Niño culmination in 2005–2006, and the maximal values were observed during the period of maximal intensity of La Niña in 2008 ($(\mathrm{ET}/\mathrm{PET})_{\mathrm{MA}} = 0.93$). Thus, monthly ET rates are relatively close to PET values during the whole year including the periods of maximal ENSO activity. The relative soil water content of the upper 30 cm horizon calculated using the Mixfor-SVAT model during the entire period of the field measurements, including the periods with maximal values of the ET / P ratio, was always higher than 80 %. This, together with the ET / PET ratio, is a clear indicator of permanently sufficient soil moisture conditions in the study area, including periods of El Niño and La Niña culminations, explaining the very low sensitivity of ΔET to ΔP.

4 Discussion

4.1 Uncertainty of the analysis

Eddy covariance flux measurements in tropical mountainous conditions are challenging. Our tower and eddy covari-

ance system was designed to minimize power consumption by using an open-path sensor, which had the consequence that rainy conditions systematically caused gaps in the flux data. To minimize a potential bias on the flux sums, we used a process-based forest model that is not biased by a lack of data in wet conditions in the same way as the statistical gap-filling algorithms often used are (Reichstein et al., 2005, see also Sect. 2.3). The weather in the tropics typically has a relatively high percentage of calm nights. The selected forest is located on a plateau in a mountainous region, and this increases the risk of CO_2-rich air draining downhill in calm nights. We investigated this effect very carefully and found that the CO_2 fluxes showed a very clear u_* threshold above which the nighttime CO_2 emission rates did not depend on u_* anymore. Using only data from nights with sufficient turbulence ($u_* > u_*$ threshold value), we minimized advection and drainage affecting the NEE estimates. Also, here we benefitted from the use of the process-based model for gap filling. We then analyzed the statistical relationships between our gap-filled monthly fluxes with climate anomaly indices and corroborated these analyses also with midday NEE data only. As time data are independent from nighttime data, we made sure that our analysis was not affected by nighttime flux loss. The correlations with midday data and ENSO indices were very similar to those with daily mean NEE data. This demonstrated the robustness of our analysis.

In addition we compared the model-predicted mean annual soil respiration rate with soil CO_2 efflux data that were measured in the study region with soil chambers (van Straaten et al., 2011). The Mixfor-SVAT model estimated an average annual soil respiration rate of $1110 \pm 30\,\mathrm{g\,C\,m^{-2}\,yr^{-1}}$ for the investigated site. This value was very close to the measured average soil CO_2 efflux of the Central Sulawesi region of $1170\,\mathrm{g\,C\,m^{-2}\,yr^{-1}}$, which shows realistic behavior of the model.

The relatively high annual NEE sums need further investigation. After applying all corrections including the correction for open-path sensor heating and after gap filling, we found an average annual uptake of $782 \pm 24\,\mathrm{g\,C\,m^{-2}\,yr^{-1}}$ (standard deviation between 5 different years). This value is higher than the range found in lowland rain forests, i.e., ranging from, e.g., 75 to $538\,\mathrm{g\,C\,m^{-2}\,yr^{-1}}$ (Luyssaert et al., 2007). The clarification of this very interesting phenomenon, maybe relating to the site history and regrowth after selected use of large individual trees by the local population, does not, however, lie within the scope of this article.

4.2 Effects of large-scale climate anomalies on carbon and water exchange in the investigated site

The main components of carbon and water balances in the tropical rainforest showed a high correlation between Nino4 and Nino3.4 SST anomalies and ΔGPP_{MA} and ΔET_{MA} values over the entire measuring period. The smoothing procedure allowed us to remove the high-frequency month-to-month oscillations in the time series of atmospheric characteristics. These are caused by local and regional circulation processes that are not directly connected with ENSO activity and thus disturb the analysis. The relationships between ΔGPP_{MA}, ΔET_{MA} and Nino4 and Nino3.4 indexes are governed via the dependency of the incoming solar radiation on ENSO development – surface water warming in Nino3.4 and 4 regions generally results in a decrease in cloudiness above the study region and thus in an increase in incoming solar radiation. The high correlation of monthly GPP and ET rates with incoming and absorbed solar radiation at this site is well described (e.g., Ibrom et al., 2008). The effects of monthly air temperature and precipitation changes on ΔGPP and ΔET variability are, on the contrary, relatively poor. ΔT_{MA}, ΔP_{MA} and ENSO intensity are not very much related.

The cross-correlation analysis (Fig. 5) shows that the ΔGPP_{MA} and ΔG_{MA} have a small 2–3 month backward shift relative to the course of Nino4 SST, i.e., the maxima in GPP_{MA} occur earlier than ENSO culmination in the central Pacific (Nino4 SST anomaly). The maximal values of ΔE_{MA} occurred simultaneously with El Niño and La Niña culminations. Such an effect of El Niño episodes on G can be explained, as mentioned above, by a decrease in the cloud cover in the region of Indonesia, due to the El Niño-associated shift in the Walker circulation cell and the corresponding zone of deep convection from the maritime continent of Indonesia toward the dateline, following SST anomaly displacement. El Niño usually begins in April, and toward August–September the ascending branch of the Walker cell leaves Indonesia and migrates eastward to the Pacific. Therefore, 3–4 months before the El Niño culmination in December–January, a decrease in cloud amount is observed over Indonesia. The weakening of El Niño, in turn, leads to a backward, westward shift in the intensive convection zone. It can result in increasing precipitation amounts in the region during the second half of the wet period after passing the maximal El Niño activity, in the gradual increase of the cloudiness, and in a decrease in incoming solar radiation. The opposite effect takes place during the La Niña with similar phase shift: simultaneously, with the spreading of a negative SST anomaly over the Pacific, the increasing of deep convection over Indonesia occurs, which results in an increase in cloudiness and precipitation, being more pronounced as it falls into the dry period of the year. The lower panels of Fig. 4 indicate, however, that the decrease in radiation due to an increase in cloudiness does not depend linearly on La Niña intensity, reaching a saturation state at approximately -20 to $-30\,\mathrm{MJ\,m^{-2}\,month^{-1}}$.

A relatively poor correlation between ΔT_{MA} patterns and ENSO activity and an insignificant influence of ΔT on ΔGPP and ΔET can mainly be explained by the small intra-annual amplitude of the air temperature in the study area not exceeding 1.0 °C as well as by the low dependence of the air temperature on incoming solar radiation. The mean monthly temperatures ranged between 19.5 and 20.5 °C in the intra-

annual development. Maximal air temperatures did not exceed 28.5 °C, even on sunny days. Such optimal thermal conditions with high precipitation amounts provide sufficient soil moistening and relatively comfortable conditions for tree growth during the whole year. As was already mentioned, even during the El Niño culmination in 2005–2006 the ET / PET did not decrease below 0.74, $(ET / PET)_{MA} > 0.81$, and the relative soil water content of the upper 30 cm horizon was always higher than 80 %.

The analysis of absolute and relative changes in GPP and ET during the periods of maximal El Niño and La Niña activities showed that GPP during the El Niño culminations of 2005 and 2007 increased by about 20 g C m^{-2} month^{-1} (6–7 %). ΔGPP_{MA} was about 9 g C m^{-2} month^{-1} (2–3 %), ΔET – about 40 mm month^{-1} (about 30 %) and ΔET_{MA} – about 10 mm month^{-1} (6–7 %). Thus, the maximal ΔGPP was 2 times lower than the mean annual amplitude of GPP (Fig. 2). The maximal ΔET was equal to the annual amplitude of ET (Fig. 2). During the La Niña culmination of 2008 the maximal relative changes in GPP were higher than the relative changes observed during El Niño events: ΔGPP was about -22 g C m^{-2} month^{-1} (8 %), ΔGPP_{MA} – about -12 g C m^{-2} month^{-1} (4 %). The maximal decrease in ΔET in the period was relatively small: ΔET decreased by about -12 mm month^{-1} (10 %) and ΔET_{MA} decreased by about -5 mm month^{-1} (4 %). ΔET was about 3 times lower than the mean annual amplitude of ET. Interestingly the radiation-dependent GPP (as represented by the smoothed 7-month mean) does not demonstrate any prolonged constant period during La Niña phases though the radiation does. During the first cold event the GPP reduction is not as strong as during the second one, although the G reductions are nearly of the same strength. It could be assumed that in the first case the effect of radiation decrease on GPP was compensated by other factors, like a slight increase in the air temperature.

Additionally, we investigated the influence of other climatic anomalies in the region on CO_2 and H_2O fluxes in the tropical rainforest, such as the Madden–Julian oscillation (MJO) and the Indian Ocean Dipole (IOD). The MJO is characterized by an eastward propagation of large regions of enhanced and suppressed deep convection from the Indian Ocean toward the central Pacific (Zhang, 2005). Each MJO cycle lasts approximately 30–60 days and includes wetter (positive) and drier (negative) phases. The outgoing long-wave radiation (OLR) measured at the top of the atmosphere is commonly used as an estimation of deep convection intensity in the tropics. It was recently shown that 6–12 months prior to the onset of an El Niño episode, a drastic intensification of the MJO occurs in the western Pacific (Zhang and Gottschalck, 2002; Lau, 2005; Hendon et al., 2007; Gushchina and Dewitte, 2011). Furthermore, MJO behavior varies significantly during the ENSO cycle: it is significantly decreased during the maxima in conventional El Niño episodes, while it is still active during the peak phase of central Pacific events. MJO rarely occurs during La Niña episodes (Gushchina and Dewitte, 2012). As MJO is strongly responsible for intra-seasonal variation of precipitation in the study region, the occurrence of MJO events was compared to the significant anomalies of the ET / P ratio and of key meteorological variables. No evidence of MJO influence is observed: the positive and negative anomalies of the ET / P ratio are associated with positive, negative and zero anomalies of OLR, filtered in the MJO interval. Also, no significant relation emerged from the correlation analysis.

Correlations between the MJO index (Wheeler and Kiladis, 1999; Gushchina and Dewitte, 2011) and the deviations of key meteorological parameters from monthly averages during the study period were very low: $r^2 = 0.03$ for T, $r^2 = 0.03$ for P and $r^2 = 0.01$ for G ($p > 0.05$, in all cases).

The IOD is characterized by changes in the SST in the western Indian Ocean, resulting in intensive rainfall in the western part of Indonesia during the positive phase and a corresponding precipitation reduction during the negative phase (Saji et al., 1999). To find a possible influence of IOD events on temporal variability in meteorological parameters and CO_2 and H_2O fluxes, the monthly mean IOD index (Dipole Mode Index, DMI) was used. Results showed that with respect to the western part of Indonesia situated close to Indian Ocean, the IOD phenomenon has no significant impact on meteorological conditions and fluxes in the area of Central Sulawesi.

Our case study showed a high sensitivity of the main components of CO_2 and H_2O fluxes in the investigated mountainous tropical rainforest in Bariri to El Niño and La Niña phenomena as well as a low sensitivity to IOD and MJO events. The time lag between the respective indices and their effect on the fluxes at our site indicates that the timing and the extent of the effects are site specific. The fluxes respond to the local weather and only indirectly to the large-scale weather anomalies, i.e., in the same way that the local weather is affected by the large-scale weather phenomena. The observed phenomena are thus not representative of all mountainous forest sites in the tropics. The conclusion is that large-scale weather anomalies do have systematic effects on local fluxes, but the timing and the extent are likely to differ across different regions.

Even though remote-sensing analyses have shown that the site is representative of the region (Ibrom et al., 2007; Propastin et al., 2012), the response to ENSO might differ in the region due to differences in altitude and land use (Erasmi et al., 2009). In general, anthropogenic deforestation has removed most parts of lowland forests so that the remaining forest cover consists mostly of mountainous forests. At the moment, there are no other FLUXNET sites situated in the equatorial mountainous rainforests of southeast Asia with which we could directly compare our findings and investigate whether a similar response to ENSO can be observed. Most of the existing FLUXNET sites (AsiaFlux) are not comparable with the investigated site as they are situated in subequatorial and tropical climate zones. These are characterized

by a higher seasonality of air temperature and precipitation compared to our equatorial site. Thus, our site provides a unique opportunity to investigative the response of an equatorial mountainous rainforest to ENSO in the western Pacific region.

5 Conclusions

CO_2 and H_2O fluxes in the mountainous tropical rainforest in Central Sulawesi in Indonesia showed a high sensitivity of monthly GPP and ET to ENSO intensity for the period from January 2004 to June 2008. This was mainly governed by the high dependency of incoming solar radiation (G) to Nino4 and Nino3.4 SST changes and the strong sensitivity of GPP and ET to G.

Interestingly, we observed time shifts between the SST anomalies and smoothed GPP anomalies driven by radiation anomalies. The maximal deviations of GPP and G from their mean values occurred 2–3 months before the peak phase of the ENSO events. The effect of ENSO intensity on RE was relatively small, mainly due to its weak effect on air temperature. In any case, the small cross correlation between RE and ENSO intensity had a compensatory effect on the respective timing of NEE, which was thus – like evapotranspiration – in synchrony with El Niño culminations. Unlike the observations at other tropical sites, precipitation variations had no influence on the CO_2 and H_2O fluxes at the study site, mainly due to the permanently sufficient soil moisture condition in the study area.

Other climatic anomalies in the western Pacific region, such as the Indian Ocean Dipole and the Madden–Julian oscillation, did not show any significant effect on either the meteorological conditions or the CO_2 and H_2O fluxes in the investigated rainforest in Central Sulawesi.

It is important to emphasize that the observation period does not cover any period with extreme El Niño events, such as, e.g., the 1982–1983 and 1997–1998 events, when the anomaly of Nino3.4 SST, during several months, exceeded 2.6 °C and more significant changes in surface water availability were observed. Also, in lowland parts of Sulawesi, characterized by higher temperatures and lower precipitation, the vegetation response to ENSO events is likely to be different and more pronounced (Erasmi et al., 2009).

All observed ENSO events during the selected period are classified as the central Pacific type. Recently, Yeh et al. (2009) showed that under projected climate change the proportion of central Pacific ENSO events might increase. Furthermore, Cai et al. (2014, 2015) showed that current projections of climate change for the 21st century suggest an increased future likelihood of both El Niño and La Niña events. Based on the results of our study, potential increases in ENSO activity would results in an increased variability in the CO_2 and H_2O exchange between the atmosphere and the tropical rainforests in these and similar regions.

Acknowledgements. The study was supported by the German Research Foundation as part of the projects "Stability of Rainforest Margins in Indonesia", STORMA (SFB 552), "Ecological and Socioeconomic Functions of Tropical Lowland Rainforest Transformation Systems (Sumatra, Indonesia)" (SFB 990) and KN 582/8-1. The Russian Science Foundation (grant RSCF 14-27-00065) supported A. Olchev during the model development.

This open-access publication was funded by the University of Göttingen.

Edited by: P. Stoy

References

Aiba, S. and Kitayama, K.: Effects of the 1997–98 El Niño drought on rain forests of Mount Kinabalu, Borneo, J. Trop. Ecol., 18, 215–230, 2002.

Ashok, K. and Yamagata, T.: The El Niño with a difference, Nature, 461, 481–484, 2009.

Ashok, K., Behera, S. K., Rao, S. A., Weng, H., and Yamagata, T.: El Niño Modoki and its possible teleconnection, J. Geophys. Res., 112, C11007, doi:10.1029/2006JC003798, 2007.

Aubinet, M., Grelle, A., Ibrom, A., Rannik, U., Moncrieff, J., Foken, T., Kowalski, A. S., Martin, P. H., Berbigier, P., Bernhofer, C., Clement, R., Elbers, J., Granier, A., Grunwald, T., Morgenstern, K., Pilegaard, K., Rebmann, C., Snijders, W., Valentini, R., and Vesala, T.: Estimates of the annual net carbon and water exchange of forests: The EUROFLUX methodology, Adv. Ecol. Res., 30, 113–175, 2000.

Aubinet, M., Vesala, T., and Papale, D. (Eds.): Eddy Covariance: A Practical Guide to Measurement and Data Analysis, Springer Atmospheric Sciences, Springer Verlag, Dordrecht, The Netherlands, 438 pp., 2012.

Burba, G. G., McDermitt, D. K., Grelle, A., Anderson, D. J., and Xu, L.: Addressing the influence of instrument surface heat exchange on the measurements of CO_2 flux from open-path gas analyzers, Global Change Biol., 14, 1854–1876, 2008.

Burba, G. G., McDermitt, D. K., Grelle, A., Anderson, D. J., and Xu, L.: Addressing the influence of instrument surface heat exchange on the measurements of CO_2 flux from open-path gas analyzers, Global Change Biol., 14, 1–23, 2012.

Cai, W., Borlace, S., Lengaigne, M., van Rensch, P., Collins, M., Vecchi, G., Timmermann, A., Santoso, A., McPhaden, M. J., Wu, L., England, M. H., Wang, G., Guilyardi, E., and Jin, F.-F.: Increasing frequency of extreme El Niño events due to greenhouse warming, Nature Climate Change, 4, 111–116, 2014.

Cai, W., Wang, G., Santoso, A., McPhaden, M., Wu, L., Jin, F.-F., Timmermann, A., Collins, M., Vecchi, G., Lengaigne, M., England, M., Dommenget, D., Takahashi, K., and Guilyardi, E.: More frequent extreme La Niña events under greenhouse warming, Nature Climate Change, 5, 132–137, 2015.

Chatfield, C.: The Analysis of Time series, An Introduction, sixth edition, Chapman & Hall/CRC, New York, 333 pp., 2004.

Chen, D. and Chen, H. W.: Using the Koppen classification to quantify climate variation and change: An example for 19012010, Environmental Development, 6, 69–79, 2013.

Ciais, P., Piao, S.-L., Cadule, P., Friedlingstein, P., and Chédin, A.: Variability and recent trends in the African terrestrial carbon balance, Biogeosciences, 6, 1935–1948, doi:10.5194/bg-6-1935-2009, 2009.

Clark, D. A. and Clark, D. B.: Climate-induced variation in canopy tree growth in a Costa Rican tropical rain forest, J. Ecol., 82, 865–872, 1994

Download Climate Timeseries: http://www.esrl.noaa.gov/psd/gcos_wgsp/Timeseries/ (last access: 2 March 2015), 24 April 2013.

Erasmi, S., Propastin, P., Kappas, M., and Panferov, O.: Patterns of NDVI variation over Indonesia and its relationship to ENSO during the period 1982–2003, J. Climate, 22, 6612–6623, 2009.

Falge, E., Reth, S., Brüggemann, N., Butterbach-Bahl, K., Goldberg, V., Oltchev, A., Schaaf, S., Spindler, G., Stiller, B., Queck, R., Köstner, B., and Bernhofer, C.: Comparison of surface energy exchange models with eddy flux data in forest and grassland ecosystems of Germany, J. Ecol. Modell., 188, 174–216, 2005.

Falk, U., Ibrom, A., Kreilein, H., Oltchev, A., and Gravenhorst, G.: Energy and water fluxes above a cacao agroforestry system in Central Sulawesi, Indonesia, indicate effects of land-use change on local climate, Meteorol. Z., 14, 219–225, 2005.

FAO: Global forest resources assessment 2010: Main report, FAO Forestry Paper 163, Rome, Italy, 340 pp., 2010.

Feely, R. A., Wanninkhof, R., Takahashi, T., and Tans, P.: Influence of El Niño on the equatorial Pacific contribution to atmospheric CO_2 accumulation, Nature, 398, 597–601, 1999.

Fisher, J. B., Sikka, M., Sitch, S., Ciais, P., Poulter, B., Galbraith, D., Lee, J.-E., Huntingford, C., Viovy, N., Zeng, N., Ahlstrom, A., Lomas, M. R., Levy, P. E., Frankenberg, C., Saatchi, S., and Malhi, Y.: African tropical rainforest net carbon dioxide fluxes in the twentieth century, Phil. Trans. R. Soc. B, 368, 20120376, doi:10.1098/rstb.2012.0376, 2013.

Gerold, G. and Leemhuis, C.: Effects of "ENSO-events" and rainforest conversion on river discharge in Central Sulawesi (Indonesia), in: Tropical Rainforests and Agroforests under Global Change Environmental Science and Engineering, edited by: Tscharntke, T., Leuschner, Ch., Veldkamp, E., Faust, H., Guhardja, E., and Bidin, A., 327–350, 2010.

Grace, J., Lloyd, J., McIntyre, J., Miranda, A., Meir, P., Miranda, H., Nobre, C., Moncrieff, J. B., Massheder, J. M., Malhi, Y., Wright, I., and Gash, J. C.: Carbon dioxide uptake by an undisturbed tropical rain forest in south-west Amazonia, 1992 to 1993, Science, 270, 778–780, 1995.

Grace, J., Malhi, Y., Lloyd, J., McIntyre, J., Miranda, A. C., Meir, P., and Miranda, H. S.: The use of eddy covariance to infer the net carbon uptake of Brazilian rain forest, Glob. Change Biol., 2, 209–218, 1996.

Graf, H.-F. and Zanchettin, D.: Central Pacific El Niño, the "subtropical bridge", and Eurasian climate, J. Geophys. Res., 117, D01102, doi:10.1029/2011JD016493, 2012.

Gushchina, D. and Dewitte, B.: The relationship between intraseasonal tropical variability and ENSO and its modulation at seasonal to decadal timescales, Central European Journal of Geosciences, 1, 175–196, doi:10.2478/s13533-011-0017-3, 2011.

Gushchina, D. and Dewitte, B.: Intraseasonal tropical atmospheric variability associated to the two flavors of El Niño, Mon. Weather Rev., 140, 3669–3681, 2012.

Hansen, M. C., Potapov, P. V., Moore, R., Hancher, M., Turubanova, S. A., Tyukavina, A., Thau, D., Stehman, S. V., Goetz, S. J., Loveland, T. R., Komardeey, A., Egorov, A., Chini, L., Justice, C. O., and Townshend, J. R. G.: High-Resolution Global Maps of 21st-Century Forest Cover Change, Science, 342, 850–853, 2013.

Hendon, H. H., Wheeler, M. C., and Zhang, C.: Seasonal Dependence of the MJO-ENSO Relationship, J. Climate, 20, 531–543, 2007.

Hirano, T., Segah, H., Harada, T., Limin, S., June, T., Hirata, R., and Osaki, M.: Carbon dioxide balance of a tropical peat swamp forest in Kalimantan, Indonesia, Glob. Change Biol., 13, 412–425, doi:10.1111/j.1365-2486.2006.01301.x, 2007.

Ibrom, A., Olchev, A., June, T., Ross, T., Kreilein, H., Falk, U., Merklein, J., Twele, A., Rakkibu, G., Grote, S., Rauf, A., and Gravenhorst, G.: Effects of land-use change on matter and energy exchange between ecosystems in the rain forest margin and the atmosphere, in: The stability of tropical rainforest margins: Linking ecological, economic and social constraints, edited by: Tscharntke, T., Leuschner, C., Zeller, M., Guhardja, E., and Bidin, A., Springer Verlag, Berlin, 463–492, 2007.

Ibrom, A., Oltchev, A., June, T., Kreilein, H., Rakkibu, G., Ross, Th., Panferov, O., and Gravenhorst, G.: Variation in photosynthetic light-use efficiency in a mountainous tropical rain forest in Indonesia, Tree Physiol., 28, 499–508, 2008.

Järvi, L., Mammarella, I., Eugster, W., Ibrom, A., Siivola, E., Dellwik, E., Keronen, P., Burba, G., and Vesala, T.: Comparison of net CO_2 fluxes measured with open- and closed-path infrared gas analyzers in urban complex environment, Boreal Environ. Res., 14, 499–514, 2009.

Kug, J.-S., Jin, F.-F., and An, S.-I.: Two types of El Niño events: Cold tongue El Niño and warm pool El Niño, J. Climate, 22, 1499–1515, 2009.

Larkin, N. K. and Harrison, D. E.: Global seasonal temperature and precipitation anomalies during El Niño autumn and winter, Geophys. Res. Lett., 32, L13705, doi:10.1029/2005GL022738, 2005.

Lau, W. K. M.: El Niño Southern Oscillation connection. Intraseasonal Variability of the Atmosphere-Ocean Climate System, edited by: Lau, W. K. M. and Waliser, D. E., Praxis Publishing, Chichester, UK, 271–300, 2005.

Lewis, S. L., Lopez-Gonzalez, G., Sonke, B., Affum-Baffoe, K., Baker, T. R., Ojo, L. O., Phillips, O. L., Reitsma, J. M., White, L., Comiskey, J. A., Djuikouo, K. M.-N., Ewango, C. E. N., Feldpausch, T. R., Hamilton, A. C., Gloor, M., Hart, T., Hladik, A., Lloyd, J., Lovett, J. C., Makana, J.-R., Malhi, Y., Mbago, F. M., Ndangalasi, H. J., Peacock, J., Peh, K. S.-H., Sheil, D., Sunderland, T., Swaine, M. D., Taplin, J., Taylor, D., Thomas, S. C., Votere, R., and Woll, H.: Increasing carbon storage in intact African tropical forests, Nature, 457, 1003–1006, 2009.

Luyssaert, S., Inglima, I., Jung, M., Richardson, A. D., Reichstein, M., Papale, D., Piao, S. L., Schulze, E.-D., Wingate, L., Matteucci, G., Aragao, L., Aubinet, M., Beer, C., Bernhofer, C., Black, K. G., Bonal, D., Bonnefond, J.-M., Chambers, J., Ciais, P., Cook, B., Davis, K. J., Dolman, A. J., Gielen, B., Goulden, M., Grace, J., Granier, A., Grelle, A., Griffis, T., Grünwald, T., Guidolotti, G., Hanson, P. J., Harding, R., Hollinger, D. Y., Hutyra, L. R., Kolari, P., Kruijt, B., Kutsch, W., Lagergren, F., Laurila, T., Law, B. E., Le Maire, G., Lindroth, A., Loustau, D., Malhi, Y., Mateus, J., Migliavacca, M., Misson, L., Montagnani, L., Moncrieff, J., Moors, E., Munger, J. W., Nikinmaa, E., Ollinger, S. V., Pita, G., Rebmann, C., Roupsard, O., Saigusa, N.,

Sanz, M. J., Seufert, G., Sierra, C., Smith, M.-L., Tang, J., Valentini, R., Vesala, T., and Janssens, I. A.: CO_2 balance of boreal, temperate, and tropical forests derived from a global database, Glob. Change Biol., 13, 2509–2537, 2007.

Malhi, Y.: The carbon balance of tropical forest regions, 1990–2005, Current Opinion in Environmental Sustainability, 2, 237–244, 2010.

Malhi, Y., Baldocchi, D. D., and Jarvis, P. G.: The carbon balance of tropical, temperate and boreal forests, Plant Cell Environ., 22, 715–740, 1999.

Moser, G., Schuldt, B., Hertel, D., Horna, V., Coners, H., Barus, H., and Leuschner, C.: Replicated throughfall exclusion experiment in an Indonesian perhumid rainforest: wood production, litter fall and fine root growth under simulated drought, Glob. Change Biol., 20, 1481–1497, doi:10.1111/gcb.12424, 2014.

Oltchev, A., Constantin, J., Gravenhorst, G., Ibrom, A., Heimann, J., Schmidt, J., Falk, M., Morgenstern, K., Richter, I., and Vygodskaya, N.: Application of a six-layer SVAT model for simulation of evapotranspiration and water uptake in a spruce forest, Phys. Chem. Earth, 21, 195–199, 1996.

Oltchev, A., Cermak, J., Nadezhdina, N., Tatarinov, F., Tishenko, A., Ibrom, A., and Gravenhorst, G.: Transpiration of a mixed forest stand: field measurements and simulation using SVAT models, J. Boreal Environ. Res., 7, 389–397, 2002.

Olchev, A., Ibrom, A., Ross, T., Falk, U., Rakkibu, G., Radler, K., Grote, S., Kreilein, H., and Gravenhorst G.: A modelling approach for simulation of water and carbon dioxide exchange between multi-species tropical rain forest and the atmosphere, J. Ecol. Modell., 212, 122–130, 2008.

Panferov, O., Ibrom, I., Kreilein, H., Oltchev, A., Rauf, A., June, T., Gravenhorst, G., and Knohl, A.: Between deforestation and climate impact: the Bariri Flux tower site in the primary montane rainforest of Central Sulawesi, Indonesia, The Newsletter of FLUXNET, 2, 17–19, 2009.

Phillips, O. L., Aragao, L., Lewis, S. L., Fisher, J. B., Lloyd, J., Lopez-Gonzalez, G., Malhi, Y., Monteagudo, A., Peacock, J., Quesada, C. A., van der Heijden, G., Almeida, S., Amaral, I., Arroyo, L., Aymard, G., Baker, T. R., Banki, O., Blanc, L., Bonal, D., Brando, P., Chave, J., de Oliveira, A. C. A., Cardozo, N. D., Czimczik, C. I, Feldpausch, T. R., Freitas, M. A., Gloor, E., Higuchi, N., Jimenez, E., Lloyd, G., Meir, P., Mendoza, C., Morel, A., Neill, D. A., Nepstad, D., Patino, S., Penuela, M. C., Prieto, A., Ramirez, F., Schwarz, M., Silva, J., Silveira, M., Thomas, A. S., ter Steege, H., Stropp, J., Vasquez, R., Zelazowski, P., Davila, E. A., Andelman, S., Andrade, A., Chao, K.-J., Erwin, T., Di Fiore, A., Honorio, C. E., Keeling, H., Killeen, T. J., Laurance, W. F., Cruz, A. P., Pitman, N. C. A., Vargas, P. N., Ramirez-Angulo, H., Rudas, A., Salamao, R., Silva, N., Terborgh, J., and Torres-Lezama, A.: Drought sensitivity of the Amazon rainforest, Science, 323, 1344–1347, 2009.

Priestley, C. H. B. and Taylor, R. J.: On the assessment of surface heat flux and evaporation using large-scale parameters, Mon. Weather Rev., 100, 81–92, 1972.

Propastin, P., Ibrom, A., Erasmi, S., and Knohl, A.: Effects of canopy photosynthesis saturation on the estimation of gross primary productivity from MODIS data in a tropical forest, Remote Sens. Environ., 121, 252–260, 2012.

Rasmusson, E. M. and Carpenter, T. H.: Variations in tropical sea surface temperature and surface wind fields associated with the Southern Oscillation/El Niño, Mon. Weather Rev., 110, 354–384, 1982.

Rayner, P. J. and Law, R. M.: The relationship between tropical CO_2 fluxes and the El Niño-Southern Oscillation, Geophys. Res. Lett., 26, 493–496, doi:10.1029/1999GL900008, 1999.

Reichstein, M., Falge, E., Baldocchi, D., Papale, D., Aubinet, M., Berbigier, P., Bernhofer, C., Buchmann, N., Gilmanov, T., Granier, A., Grunwald, T., Havrankova, K., Ilvesniemi, H., Janous, D., Knohl, A., Laurila, T., Lohila, A., Loustau, D., Matteucci, G., Meyers, T., Miglietta, F., Ourcival, J.-M., Pumpanen, J., Rambal, S., Rotenberg, E., Sanz, M., Tenhunen, J., Seufert, G., Vaccari, F., Vesala, T., Yakir, D., and Valentini, R.: On the separation of net ecosystem exchange into assimilation and ecosystem respiration: review and improved algorithm, Global Change Biol., 11, 1424–1439, 2005.

Reverter, B. R., Carrara, A., Fernández, A., Gimeno, C., Sanz, M. J., Serrano-Ortiz, P., Sánchez-Cañete, E. P., Were, A., Domingo, F., Resco, V., Burba, G. G., and Kowalski, A. S.: Adjustment of annual NEE and ET for the open-path IRGA self-heating correction: Magnitude and approximation over a range of climate, Agr. Forest Meteorol., 151, 1856–1861, 2011.

Saji, N. H., Goswami, B. N., Vinayachandran, P. N., and Yamagata, T.: A dipole mode in the tropical Indian Ocean, Nature, 401, 360–363, 1999.

Setoh, T., Imawaki, S., Ostrovskii, A., and Umatani S.: Interdecadal Variations of ENSO Signals and Annual Cycles Revealed by Wavelet Analysis, J. Oceanography, 55, 385–394, 1999.

van Straaten, O., Veldkamp, E., and Corre, M. D.: Simulated drought reduces soil CO_2 efflux and production in a tropical forest in Sulawesi, Indonesia, Ecosphere, 2, art119, doi:10.1073/pnas.1504628112, 2011.

Wang, C.: Atmospheric circulation cells associated with the El Niño-Southern Oscillation, J. Climate, 15, 399–419, 2002.

Wheeler, M. C. and Kiladis, G. N.: Convectively coupled equatorial waves: Analysis of clouds and temperature in the wavenumber–frequency domain, J. Atmos. Sci., 56, 374–399, 1999.

Yeh, S.-W., Kug, J.-S., Dewitte, B., Kwon, M.-H., Kirtman, B., and Jin, F.-F.: El Niño in a changing climate, Nature, 461, 511–514, 2009.

Yuan, Y. and Yan, H.: Different types of La Niña events and different responses of the tropical atmosphere, Chinese Sci. Bull., 58, 406–415, 2013.

Zhang, C.: Madden-Julian Oscillation, Rev. Geophys., 43, RG2003, doi:10.1029/2004RG000158, 2005.

Zhang, C. and Gottschalck, J.: SST Anomalies of ENSO and the Madden–Julian oscillation in the equatorial Pacific, J. Climate, 15, 2429–2445, 2002.